Jurnal Teknologi, 48(D) Jun 2008: 75–89

STARFRUIT SHAPE DEFECT ESTIMATION BASED ON CONCAVE AND CONVEX AREA OF A CLOSED PLANAR CURVE

MUSA MOKJI[1] & S.A.R. ABU BAKAR[2]

Abstract. In this paper, a shape representation based on concave and convex area along a closed curve is presented. The proposed technique involves the process of the curvature estimation from the input curve and search for its corresponding critical points. By splitting the critical points into concave and convex categories, the concave and convex area are computed. From these statistical features, two problems related to the shape (curve) are investigated. Here, the proposed technique is tested on shape defect estimation and shape recognition of starfruit. In the first case, defect is measured by computing concave energy, which is proportional to the defect. For shape recognition, starfruit's stem is identified and removed from the starfruit's shape, as it will contributes false computation of defect measurement. For both cases, the proposed technique is tested with three different curvature estimation techniques to validate the results.

Keywords: Shape representation, curvature, critical point, concave and convex area

Abstrak. Dalam kertas kerja ini, sebuah perwakilan bentuk berdasarkan kawasan cekung dan cembung di sepanjang keluk tertutup dipersembahkan. Teknik yang dicadangkan dalam kertas kerja ini melibatkan proses anggaran kekelukan daripada keluk masukan dan juga proses pencarian titik kritikal pada keluk masukan tersebut. Dengan mengasingkan titik kritikal tersebut kepada kategori cekung dan cembung, pengiraan kawasan cekung dan cembung dilakukan. Daripada ciri-ciri statistik ini, dua permasalahan berkaitan dengan bentuk disiasat. Di sini, teknik yang dicadangkan diuji terhadap proses penganggaran kerosakan bentuk dan pengenalan bentuk pada buah belimbing. Pada kes pertama, kerosakan bentuk belimbing diukur dengan mengira kuasa cekung di mana kuasa cekung ini adalah selanjar dengan kerosakan bentuk tersebut. Untuk kes pengenalpastian bentuk pula, tangkai belimbing adalah objek untuk dikenal pasti dan tangkai belimbing ini akan diasingkan daripada bentuk belimbing kerana ia akan menyumbang kepada kesalahan pengiraan kerosakan bentuk belimbing. Bagi kedua-dua kes, teknik yang dicadangkan diuji dengan tiga teknik penganggaran kekelukan untuk memastikan keberkesanan teknik yang dicadangkan.

Kata kunci: Perwakilan bentuk, kekelukan, titik kritikal, kawasan cekung dan cembung

1.0 INTRODUCTION

Shapes play a fundamental role in understanding objects in terms of their behavior and characteristics, such as their identity and functionality. Thus, representing shapes

[1&2]Faculty of Electrical Engineering, Universiti Teknologi Malaysia
Email: musa@fke.utm.my, syed@fke.utm.my

as mathematical model is emerging as a major area of research, which impacts diverse applications ranging from image analysis and pattern recognition to computer graphics and computer animation. Local shape descriptor will characterizes the image content in the surroundings of a point. The value of a pixel in a gray level image can be considered as the simplest type of local shape descriptor. Local shape descriptor can also indicate the presence of feature, often called a salient feature, such as an edge, a corner, or a specific type of junction at a given location in the image. In this paper, a shape defect detection and recognition technique based on curvature of a planar curve is presented. The aim is to build a set of descriptor of an object using local shape information and to extract a global set of attributes that can be used for shape defect detection and recognition in starfruit quality inspection process. Here, new features called concave and convex area will be generated as the shape descriptor.

Shape representation technique can also be categorized based on the input representation form. Here, the techniques are divided into region-based technique, which extract information from the whole region of the object and contour-based technique, which is based on the boundaries of the object [16]. However, a combination of both techniques is implemented in constructing the proposed features (concave and convex area). Here, the *concave* and *convex* terms are derived from the contour-based technique and the *area* term is referring to the region-based technique.

In the region-based technique, simple shape of object can be represented by its geometric features (rectangularity, elongatedness, direction, compactness and etc.) and statistical measure. However, for more complex image, the object must be represented by a planar graph where each point on the graph will represents a sub-region of simple shape of the object resulting from region decomposition [14]. Geometric representation only works for simple object as it only gives global information. For complex objects, which contain significant local attributes needs a more complex technique. However, there is a more reliable but less complicated technique, which is based on the statistical features of the object. It is called Moment Invariant. In 1992, Hu [6] has introduced seven rotation, translation and scale invariant moment characteristics. Hu's moment invariant is proven to be very useful in many applications [19, 24]. Thus, its characteristics are also discussed in many publications [2, 8]. Although moment invariant has good characteristic describing shape of an object, its description is still based on the global information and lack of the local information. Thus, the statistical information extracted using moment invariant is not sufficient for the starfruit shape defect estimation where the requirement for the local information is crucial.

In region-based technique, local information from an object can be best described by region decomposition into smaller and simpler sub-regions. The object's shape can then be described by the properties from the set of all the sub-regions. The decomposition approach is based on the idea that shape of an object is hierarchically constructed from primitive shapes, which are the simplest element that form the

complete shape region. Triangle, square, circle and convex shapes are the examples of the primitive shapes. Normally, the decomposed image is represented in tree structure as applied by J. M. Reinhardt and W. E. Higgins [13]. Another method of shape decomposition is based on convex hull computation [22, 23]. Convex hull is the smallest convex region that consists of all the curve points. To achieve an efficient computation of the convex hull, many linear-time convex hull detection algorithms have been introduced. However, more than half of them were later discovered to be incorrect [20, 21]. The first linear-time algorithm that has been proved to be correct was presented by McCallum and Avis [11].

Either one of the shape decomposition algorithm discussed previously can be very useful in extracting the local information for the defect estimation of the starfruit. Nevertheless, these decomposition techniques based on region are computationally expensive and have complex algorithm. On the other hand, simpler technique of extracting the local information can be obtained using the contour-based technique. In the contour based technique, shape information is extracted along the boundary of the object where both local and global information exist. The simplest contour-based technique is by representing the object's shape based on chain code. The chain code is also known as Freeman's code where it describes shapes by a sequence of unit-size line segments with a given orientation [16]. In other words, chain code sets a code (orientation) for each of the adjacent curve points. A chain code is very sensitive to noise, scale and rotation. Thus, a smoothed version of the chain code as applied in [10] will have a better representation of the shape.

Although chain code representation is simple, however it does not contain enough information for the starfruit defect estimation. Apart from the chain code, a better representation based on geometric features of the shape can gives more information. The geometric features that can be extracted from an object's boundary are such as *boundary length*, *curvature*, *signature* and *chord distribution* [16]. *Boundary length* is a feature that describes global measure and can be simply derived from the chain code representation. The second feature, *curvature*, is a local measure of the object that represents boundary as the rate of slopes change. From the curvature, another two features can be derived, which are critical points or also called corner points on the objects boundary (local measure) and bending energy (global measure). The other two features, *signature* and *chord distribution* are also local measure. *Signature* is defined as a sequence of normal contour distance between two curve points and *chord distribution* computes the length of line joining any two curve points. The disadvantage of signature is its complex computation while chord distribution is difficult in determining the best reference points in its computation. Many other methods and approach can be used to describe shape based on its contour. Most of them have excellent shape description abilities but on the other hand they have complicated computation [15]. As an example, B-spline representation applied polynomial in its computation. Another example is a technique called Hough

transform where locations and orientations of certain types of line are identified in a digital image. Hough transform has been introduced by Paul Hough in 1962 and then modified by Richard Duda and Peter Hart in 1972 [9]. The technique is very computationally expensive as each of the curve points need to be transform into a planar curve.

Based on the simplicity and local information embedded in the curvature representation technique, this technique is chose to be implemented in the starfruit shape defect estimation. From the curvature computation, boundary of the starfruit shape will be categorized into concave and convex. Then, based on the region-based technique of the shape representation, the area of the concave and convex are computed to estimate the starfruit shape defect. The rest of this paper will discuss these processes. Curvature computation is presented in subtopic two. Then, in subtopic three, a feature called critical point that is derived from the curvature is discussed. The proposed features, which are the concave and convex area, are finally discussed in subtopic four. At the end of the discussions, performance of the proposed method is measured based on three different curvature estimation techniques.

2.0 DIFFERENTIAL GEOMETRY OF PLANAR CURVE

Let the smooth planar curve is given as $C(t) = [x(t), y(t)]$ with the number of points $0 \le t \le b$ where $x(t)$ and $y(t)$ correspond to a pair of points in 2-dimensional coordinate plane and b is the end curve point. $C(t)$ or its discrete form $C(n)$ is extracted from the input image using 8-connectivity chain code technique measured as multiples of 45° counter clockwise direction change. The original output of the chain coded curve is in 1-dimensional data code. Thus, the code is translated into the coordinate form to obtain the 2-dimensional data of $C(n) = [x(t), y(n)]$. Second derivative of the curve $C(n)$, which is invariant to rotation, contributes to a measure called curvature. Curvature is estimated at each of the curve point by taking the angular difference between its slopes [5], which is given as

$$\kappa(t) = \frac{\dot{x}(t)\,\ddot{y}(t) - \dot{y}(t)\,\ddot{x}(t)}{\left(\dot{x}(t)^2 + \dot{y}(t)^2\right)^{3/2}} \tag{1}$$

For a discrete curve, which is used in this work, its tangent vector and curvature measure will produce discrete values. Discrete tangent vector and curvature does not show its real behavior at each of the curve points. This is because in discrete space, the smoothness of the curve has been violated. Thus, the curvature description must be slightly modified to overcome the problem. This can be done by estimating the curvature by applying curve fitting techniques to the curve or directly from the curve points [16]. Curve fitting involves expensive computations [4], which is not the

interest of this work. For non-curve fitting techniques, usually the curve is subjected to Gaussian smoothing or moving cord estimation. Gaussian smoothing approach typically adopts the continuous definitions of tangent and curvature for the discrete case. For example, Mokhtarian and Mackworth [12] defined curvature as

$$\kappa(u,\sigma)=\frac{\dot{X}(u,\sigma)\ddot{Y}(u,\sigma)-\dot{Y}(u,\sigma)\ddot{X}(u,\sigma)}{\left(\dot{X}(u,\sigma)^2+\dot{Y}(u,\sigma)^2\right)^{3/2}} \tag{2}$$

where

$$\dot{X}(u,\sigma)=x(u)\otimes\dot{g}(u,\sigma),\qquad \ddot{X}(u,\sigma)=x(u)\otimes\ddot{g}(u,\sigma)$$
$$\dot{Y}(u,\sigma)=y(u)\otimes\dot{g}(u,\sigma),\qquad \ddot{Y}(u,\sigma)=y(u)\otimes\ddot{g}(u,\sigma)$$

In Equation 2, it shows that the input curve is convolved with a Gaussian operator $g(u, \sigma)$. Another example is the work reported in [1]. A simpler version of this type of curvature estimation is by replacing the Gaussian operator with mean operator [17]. In Gaussian smoothing, unnecessary details are removed, however this also changes the shape and removes the corners, unless adaptive smoothing [25] is applied. Besides, the choice of a suitable σ (standard deviation) is too dependent on its input curve. There is no single σ that suits all curve shapes. Due to this difficulty, a technique called multi-scale curvature is proposed such as the work presented in [5]. This technique produces better results as curvature is measured at multiple σ. A major disadvantage of the multi-scale computation is that it is computationally expensive. Instead of using the coordinate form curve, the curvature can also be estimated using the input curve in the chain code form [14]. It is measured by taking the first derivative of the chain code data and convolves with the Gaussian operator as shown in Equation 3. This requires only one stage of derivative as the chain code data itself already represents the first derivative (slope) of the input curve. Even though the equation seems to be simpler than the coordinate form based equation (Equation 2), however, curve represents in the coordinate form is more suitable for our proposed method, which will be discussed in subsequent topics.

$$\kappa(n)=\dot{C}(n)\otimes g(u,\sigma) \tag{3}$$

In moving chord estimation technique, the curvature is approximated based on a set of straight lines between two curve points, namely chord. This technique is simple to implement, fast to execute and provides greater smoothing effect than Gaussian filters [7]. Nevertheless, this technique is sensitive to noise. A second smoothing is usually applied. The choice of the chord length will determine its outcome and the suitable chord length, which depends on the input curve pattern. Thus, as Gaussian smoothing technique requires the right s for the best result, moving chord estimation technique requires the right chord length. For example, Han and Poston [5]

approximated curvature by distance accumulation on the moving chord using various chord lengths.

3.0 CRITICAL POINTS

Previous section has stated that curvature is sensitive to noise and many approaches have been applied in order to improve the discrete curvature estimation. Thus, this attribute is not robust for describing shape characteristic or even if it does, it includes complex and computationally expensive processes. In curvature, there exist local attributes called critical points. These points are corner points on curve where curvature value is at maximum or minimum [16]. An interesting fact is, these critical points provide better robustness. Normally, the curvature is differentiated to obtain these points. In other words any neighbor point that changes in sign is considered as critical point. Most of the previous work [12, 25, 7] also set a threshold value to eliminate unwanted critical points. For advance work searching for the critical points, Zhu and Chirlian [25] improved the technique from scale-space curvature by applying nonlinear approach, which has less computation burden. Teh and Chin [18] came out with a technique that searches for critical points without relying on the knowledge of any special properties of the input pattern and create scale, rotation and translation invariant attributes. A few other examples are described in [1, 3]. These work involve complex algorithm, which is not the interest in this paper.

Now, let p be a curve point and S be a set of curve point or simply a curve. Then, let $\tilde{p}$ be a critical point and C be a set of the critical point. As the critical points are part of the curve, we have $C \subset S$. Applying threshold value τ to the curvature $\kappa(p)$ as in the [12, 25, 7], critical point search along the curve is now limited to a set of points $T(q)$, which is a set of curve point S when $\kappa(p)$ is restricted with τ and $q \leq p$ where $C \subset T$. The critical points is then determined as the points occur at the zero crossing spot of the first derivative of $T(q)$. Figure 1 illustrates the critical points search processes and Figure 2 shows the search result for critical points using Mokhtarian and Mackworth, Han and Poston and mean curvature estimation

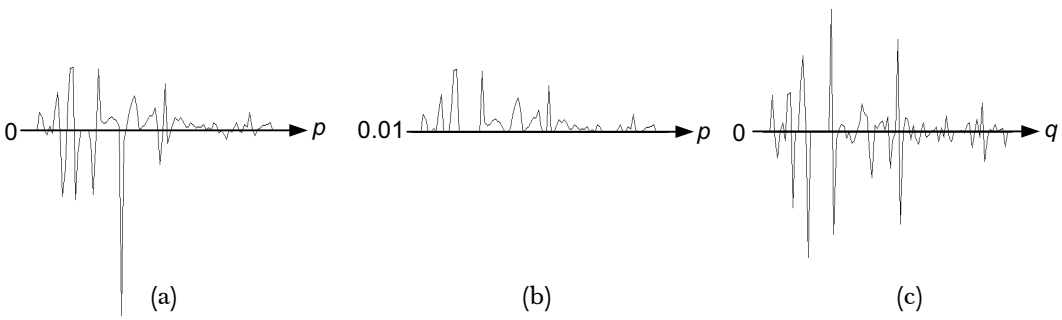

Figure 1 Critical points search processes. (a) Curvature $\kappa(p)$, (b) $\kappa(p) > 0.01$, (c) $T(q)$

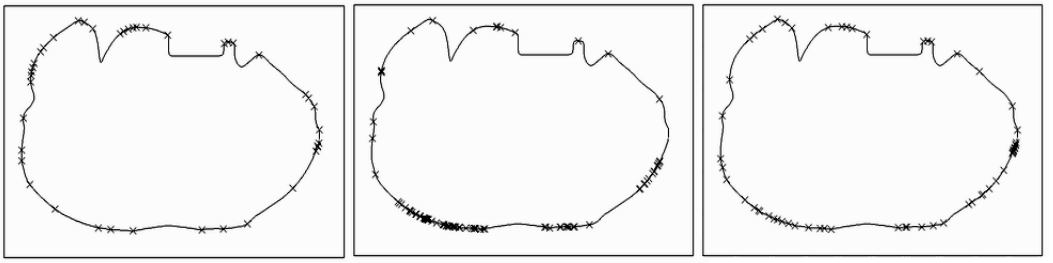

(a) (b) (c)

Figure 2 Critical points. (a) Mokhtarian and Mackworth (b) Han and Poston (c) Mean curvature estimation [x – critical point]

technique with $\kappa(p) > 0.01$. Input curve for the critical points searched in Figure 1 is referring to the image shown in Figure 2.

Critical points C in Figure 2 only occurs on the convex of the curve as $\kappa(p)$ is limited to positive values. Most of the critical points are positioned almost at similar position across the three figures. However, the number of critical points in each curve area is irregular. This is due to the noisy curvature. A better result for critical point positioning can be obtained by changing its threshold value τ. However, deciding which the most suitable τ value is subjective. A higher τ is more suitable for deep concave and convex while a lower τ is suitable for shallow concave and convex.

4.0 CONCAVE AND CONVEX AREA

Based on Figure 2, as the critical points are still noisy even after threshold is applied to the curvature computation, this paper proposes a computation of concave and convex area between two critical points to reduce the noise effect. Concave and convex area is defined as an area between a straight line Y and curve S where both are bounded by two adjacent critical points. The straight line Y joining the two critical points is also called chord.

To compute both the concave and convex area that lies on the input curve, the first step is to categorize the curve point into concave and convex. Categorizing between concave and convex point on the curve can be done directly from the curvature value. Curve point with positive curvature value represents a convex point while curve point with negative curvature value represents a concave point. As critical points carry out $C \subset S$, thus the critical points can also be divided into concave and convex critical points. Categorizing the critical point is also simple where all convex critical points only occur on convex curve point (positive curvature) and vice versa. These critical points should also follow the following equations

$$C^{+} \cap C^{-} = 0 \tag{4}$$

$$C^{+} \cup C^{-} = 0 \tag{5}$$

C^{+} and C^{-} are denoted by a set of convex critical point and a set of concave critical point accordingly. Previously, a curve is defined by $S(p)$. Writing it in coordinate form, $S(p) = \{S_x(p), S_y(p)\}$. Also, for C^{+} and C^{-}, they can be written as $C^{+}{}_i = \{C^{+}{}_{xi}, C^{+}{}_{yi}\}$ and $C^{-}{}_j = \{C^{-}{}_{xj}, C^{-}{}_{yj}\}$ where i & $j < p$. As critical points have been divided into concave and convex point, they will be treated separately.

Concave and convex area can be computed by taking an area under the curve towards the chord, which both are bounded by two adjacent critical points. In coordinate form, if both the bounded curve and the chord are rotated and translated until its start point and end point reach coordinate-x or both points lies on the horizontal line, the concave or convex area can be written as

$$A = \int S'(p) \partial p \tag{6}$$

or it is approximated by a summation form as

$$A = \sum_{p=\tilde{p}}^{\tilde{p}+1} S'(p) \tag{7}$$

where $S'(p)$ is the rotated and translated curve $S(p)$. In geometry form, $S'(p)$ is known as the length between the curve points to the line Y perpendicularly. With this circumstance, $S'(p)$ can be represented using linear equation, which is denoted by

$$S'(p) = L(p) = \ell(p) \sin \theta \tag{8}$$

where

$$\ell(p) = S_y(p) = m_i S_x(p) - c_i \tag{9}$$

Equation 9 computes the length vertically and this length is rotated perpendicularly to the chord by sin θ where θ is the angle between the vertical line and the perpendicular line and it is defined as

$$\theta = \frac{\pi}{2} - \left|\tan^{-1}(m)\right| \tag{10}$$

As in the common linear equation for a straight line, m_i and c_i is referred to gradient and y-axis intercept. They are measured between two adjacent critical points. Thus we have

$$m_i = \frac{C_{yi}^{+} - C_{y(i+1)}^{+}}{C_{xi}^{+} - C_{x(i+1)}^{+}} \tag{11}$$

$$c_i = C_{yi}^{+} - m_i C_{xi}^{+} \tag{12}$$

Note that indexes used in Equation 11 and Equation 12 are i and '+' sign. This means that they are referring to convex critical point. For concave critical points, i is replaced with j and '+' sign is replaced with '–' sign. Graphically, all these computation are illustrated in Figure 3. In the computation of A, as concave and convex are treated separately, each computation picks only one type of the critical point, whether they are concave critical points or convex critical points. Specifically, convex critical point is used for concave area computation and concave critical point is applied in order to compute convex area.

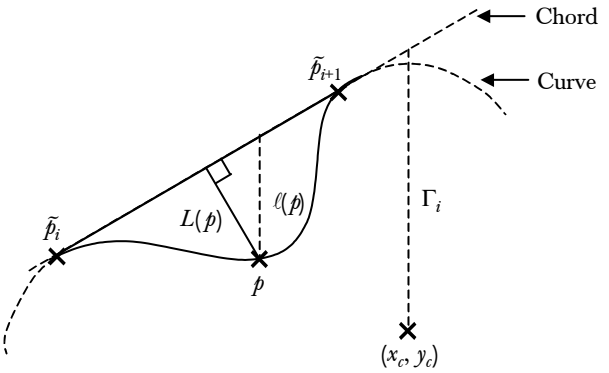

Figure 3 Concave and convex area computation

Once the right critical points are selected and $L(p)$ is computed based on Equation 8, which includes both positive and negative values. However, only one part of the values is considered in the computation because a wrongly picked sign value will result in a wrong computation. For an example, if concave area is computed, picking false sign value will lead to the computation of convex area but not concave area as it suppose to. Thus, a variable Γ is introduced to determine the correct value to be picked, either the positive or negative values. Γ is determined as the length from the center of the closed curve to the current chord. Here, the center of the closed curve is represented by $\{x_c, y_c\}$ and illustrated in the partial closed curve in Figure 3. Thus

$$\Gamma_i = y_c - m_i x_c - c_i \tag{13}$$

Redefining Equation 7 for its positive and negative value, we have

$$A(\tilde{p}) = \sum_{p=\tilde{p}}^{\tilde{p}+1} L^{+ve}(p) + \sum_{p=\tilde{p}}^{\tilde{p}+1} L^{-ve}(p) \tag{14}$$

and by adopting Γ to the equation in order to choose only the correct value will yield a separate equation for concave and convex area.

$$A_{concave}(\tilde{p}) = \begin{cases} \sum_{p=\tilde{p}}^{\tilde{p}+1} L^{+ve}(p) & if\ \Gamma > 0 \\ \sum_{p=\tilde{p}}^{\tilde{p}+1} L^{-ve}(p) & f\ \Gamma \le 0 \end{cases} \tag{15}$$

and

$$A_{convex}(\tilde{p}) = \begin{cases} \sum_{p=\tilde{p}}^{\tilde{p}+1} L^{+ve}(p) & if\ \Gamma < 0 \\ \sum_{p=\tilde{p}}^{\tilde{p}+1} L^{-ve}(p) & f\ \Gamma \ge 0 \end{cases} \tag{16}$$

The only difference between concave area and convex area is the sign of the Γ value, which is contrary to each other. Figure 4 shows the plot of both concave area ($A_{concave}$) and convex area (A_{convex}) with respect to the curve points position (p) for several different method using the input curve taken from Figure 2.

Results in Figure 4 shows that all the three techniques are able to produce an approximately similar output, although critical points tracked between these

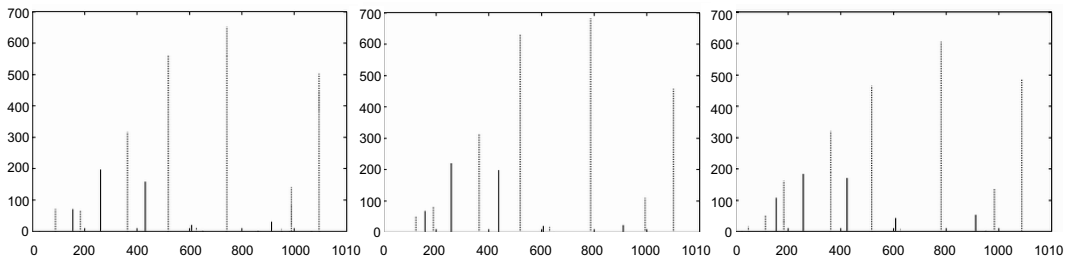

Figure 4 Concave and convex area (a) Mokhtarian and Mackworth (b) Han and Poston (c) Mean curvature estimation [--- convex area —— concave area]

techniques (Figure 2) seems to be irregular. This is because neighboring critical points with close distance will results in a very small area value. Besides, based on Equation 15 and Equation 16, two adjacent convex (concave) critical points with no concave (convex) points in between them will results a zero value. Hence, only adjacent critical points with deep enough concave or convex between them are visible in the computation. Thus, by splitting the computation into two parts (concave and convex), a more robust attribute is obtained.

5.0 EXPERIMENTAL RESULTS

In order to test the reliability of the proposed method, the method was tested on two cases. First, it was tested to estimate the shape defects on a starfruit. The second case was to recognize a plain shape. Shape information on starfruit is important, as it will determine its quality. Good shaped starfruits will attract more people to buy and is suitable as decoration for hotel style food and drink. Shape defect occurs on a starfruit is mainly caused by bugs and soil composition. However it is not the intention of this work to overcome this problem. However this paper concentrates more on measuring the amount of the shape defect. Later, the measure will be used as guidance for grading process.

Samples used in this experiment are taken by capturing starfruits images with digital camera. From the starfruit images, the shape of the starfruit is extracted using chain-code algorithm. As a result, closed curves containing concave and convex is obtained representing the starfruit shape. In the first test, shape defect on the starfruit is represented by the concave. Thus, the shape defect can be measured based on the concave area ($A_{concave}$). Here, a global attribute called concave energy, which is defined as the sum of concave area along the closed curve is computed. Figure 5

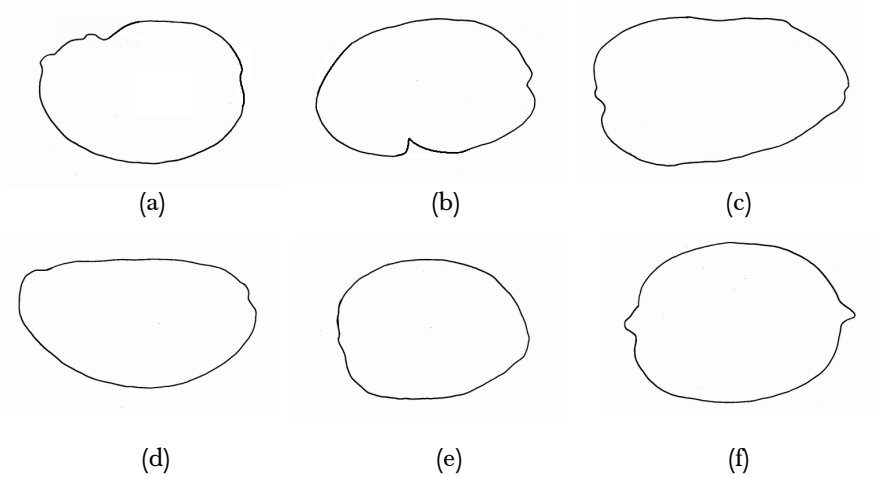

Figure 5 Starfruit shape samples

shows six shapes of starfruit, which are used in the experiment. The starfruit shapes (a – d) are defective, while shape (e – f) are defects free. The experimental results are shown in Table 1.

Table 1 Shape defect result based on concave energy

		Concave Energy		
Shape	τ	**Mokhtarian & Mackwoth**	**Han & Poston**	**Averaging Filter**
A	0	498	501	480
	0.005	513	500	491
	0.01	520	506	500
B	0	650	670	695
	0.005	690	691	713
	0.01	749	700	760
C	0	480	510	493
	0.005	500	513	496
	0.01	500	520	508
D	0	111	90	108
	0.005	110	100	110
	0.01	113	100	120
E	0	15	9	10
	0.005	15	9	11
	0.01	15	10	11
F	0	14	18	14
	0.005	15	18	16
	0.01	22	20	22

Table 1 shows that the concave energy of shape a, b, c and d are higher compared to the shape d and e as they contain some defects. This means that the concave energy is proportional to the defect amount. Table 1 also shows the results for three different values of τ, which represent different number of critical points tracked along the closed curve. An increase in τ will decrease the number of critical points. The results across those three values of τ did not vary significantly as expected. However, if the defect's computation of those six samples are based on the total of critical points occurred along the concave, unstable values across the three technique are produced as shown in Table 2.

Table 1 and Table 2 show that although unstable or various placement of the critical point exist along the curve (Figure 2), computation of concave energy results a more stable measure compared to the technique based on the critical points.

The algorithm is also tested on another 100 samples of starfruits to classify them whether the starfruit has a healthy shape or vice versa. Starfruit shapes that have less than 10% of the concave area within the whole starfruit shape area are considered as

Table 2 Shape defect result based on critical points

		Concave Energy		
Shape	τ	**Mokhtarian & Mackwoth**	**Han & Poston**	**Averaging Filter**
A	0	321	450	300
	0.005	207	301	183
	0.01	152	163	114
B	0	286	364	244
	0.005	153	191	107
	0.01	84	87	72
C	0	318	407	293
	0.005	186	281	166
	0.01	115	144	88
D	0	332	400	280
	0.005	180	267	160
	0.01	98	111	81
E	0	93	120	98
	0.005	85	100	63
	0.01	47	63	27
F	0	101	124	96
	0.005	83	110	77
	0.01	62	73	34

healthy. To determine the accuracy of the classification, a cross validation with human vision is made. It is found that the accuracy result based on Mohtarian & Mackwoth curvature is 94%, while 90% and 93% are obtained for Han & Poston curvature and averaging filter curvature accordingly.

Next, the algorithm is tested for plain shape recognition. In this case, the algorithm will recognize stem in the starfruit. Stem in a starfruit will cause a wrong computation of the defect estimation. Thus, once the stem has been recognized, it can be ignored in the defect estimation computation. In this case, convex area is used as a descriptor. Additionally, another feature is considered to strengthen the algorithm. It is distance between the neighboring critical points as defined in the Equation 17.

$$d(\tilde{p}) = \left(\left[C_x(\tilde{p}) - C_x(\tilde{p}+1) \right]^2 + \left[C_y(\tilde{p}) - C_y(\tilde{p}+1) \right]^2 \right)^{1/2} \tag{17}$$

Using empirical method, threshold for $d(\tilde{p})$ and $A_{convex}(\tilde{p})$ is chosen in order to identify the stem shape. Here, a convex on the starfruit curve shape is considered as stem if $d(\tilde{p}) \leq 10$ and $A_{convex}(\tilde{p}) \geq 50$. The previous sample set is used for testing. In the sample set, there are 60 samples without the stem and 40 samples with the stem. The experimental results are shown in Table 3, which calculate the accuracy of true identification.

Table 3 Accuracy of stem recognition

	With stem	**Without stem**
Mokhtarian & Mackwoth	92.5%	98.33%
Han & Poston	87.5%	100%
Averaging Filter	90%	98.33%

From Table 3, it is shown that the accuracy for the recognition of samples without the stem is better compared to samples with the stem. The reason for the incorrectly recognized samples with the stem is due to the short size of the stem, which does not significantly influence the defect estimation. However, the recognition sensitivity of the stem can be improved by increasing the threshold for $d(\tilde{p})$ and $A_{convex}(\tilde{p})$.

6.0 CONCLUSION

We have presented a method based on concave and convex area computation as a descriptor for shape representation. The technique manipulates noisy critical points into the proposed features, which are more stable. This is done by splitting the critical points into concave and convex critical points and computes the concave and convex area. The proposed technique has the ability to prevent wrong computation of the unwanted critical points. Thus a more stable result can be obtained. The algorithm is tested based on three curvature estimation techniques. It shows that concave and convex area computation based on these techniques give stable values, which are proportional to the shape defect of the starfruit. Good results also obtained in identifying the stem shape.

REFERENCES

[1] Angelopoulou, E. and L. B. Wolff. 1998. Sign of Gaussian Curvature from Curve Orientation in Photometric Space. *IEEE Trans. Pattern Ana. & Machine Intellig.* 20(10): 1056-1066.

[2] Chen, Y., M. Zhang, P. Lu and Y. Wang. 2005. Local Moment Invariant Analysis. *Int. Conf. on Computer Graphics, Imaging and Vision: New Trends.* 137-140.

[3] Fischler, M. A. and H. C. Wolf. 1994. Locating Perceptually Salient Points on Planar Curves. *IEEE Trans. on Pattern Analysis and Machine Intelligence.* 16(2): 113-129.

[4] Flynn, P. J. and A. K. Jain. 1989. On Reliable Curvature Estimation. *Proc. of IEEE Computer Society Conf. on Computer Vision & Pattern Recognition.* 110-116.

[5] Han, J. H. and T. Poston. 1993. Distance Accumulation and Planar Curvature. *Proc. of Fourth International Conference on Computer Vision.* 487-491.

[6] Hu, M-K. 1992. Visual Pattern Recognition By Moment Invariants. *IRE Trans. on Information Theory.* IT-8: 179-187.

[7] Ip, H. H. S. and W. H. 1997. Wong. Fast Conditioning Algorithm for Significant Zero Curvature Detection. *IEE Proc. on Vision, Image & Signal Proc.* 144(1): 23-30

[8] Jain, A. K. 1989. *Fundamentals of Digital Image Processing*. NJ: Prentice-Hall, Englewood Cliffs.

[9] Jia, C. L., K. F. Ji, Y. M. Jiang and G. Y. Kuang, 2005. Road Extraction from High-Resolution SAR Imagery Using Hough Transform. *IEEE Int. Geoscience & Remote Sens. Symp.* 1:4-9.

[10] Li, X. and Z. Zhiying. 1988. Group Direction Difference Chain Codes for the Representation of the Border. *SPIE Trans. Digital & Opt. Shape Rep. and Pattern. Recog.* 372-376.

[11] McCallum, D. and D. Avis. 1979. A Linear Algorithm for Finding the Convex Hull Of a Simple Polygon. *Information Processing Letters.* 9: 201-206.

[12] Mokhtarian, F. and R. Suomela. 1998. Robust Image Corner Detection Through Curvature Scale Space. *IEEE Trans. on Pattern Analysis & Machine Intelligence.* 20(12): 1376-1381.

[13] Reinhardt, J. M. and W. E. Higgins. 1996. Comparison Between the Morphological Skeleton & Morphological Shape Decomposition. *IEEE Trans. on Pattern Ana. & Machine Intellig.* 18(9): 951-957.

[14] Rosenfeld, A. 1979. *Picture Languages - Formal Models for Picture Recognition*. New York: Academic Press.

[15] Saint-Marc, P., H. Rom and G. Medioni. 1993. B-spline Contour Representation and Symmetry Detection. *IEEE Trans. on Pattern Analysis & Machine Intelligence*. 15(11): 1191-1197.

[16] Sonka, M., V. Hlavac and R. Boyle. 1999. *Image Processing, Analysis and Machine Vision. 2nd Edition*. Boston: Thomson-Engineering.

[17] Surazhsky, T., E. Magid, O. Soldea, G. Elber and E. Rivlin. 2003. A Comparison of Gaussian and Mean Curvatures Estimation Methods on Triangular Meshes. *IEEE Int. Conf. on Robotics and Automation.* 1: 1021-1026.

[18] Teh, C. H. and R. T. Chin. 1989. On the Detection of Dominant Points on Digital Curves. *IEEE Trans. on Pattern Analysis and Machine Intelligence.* 11(8): 859-872.

[19] Tianxu, Z. and L. Jin. 2004. Blurred Image Recognition Based on Complex Moment Invariants. *Int. Conference on Image Processing.* 3: 2131-2134.

[20] Toussaint, G. 1985. A Historical Note on Convex Hull Finding Algorithms. *Pattern Recognition Letters.* 3(1): 21-28.

[21] Toussaint, G. 1991. A Counter-Example to a Convex Hull Algorithm for Polygons. *Pattern Recognition Letters.* 24(2): 183-184.

[22] Wilson, G. R. and B. G. Batchelor. 1989. Convex Hull of Chain-Coded Blob. *IEE Proc. on Computers and Digital Techniques.* 136(6): 530-534.

[23] Yang, Z. and F. S. Cohen. 1999. Image Registration & Object Recognition Using Affine Invariants and Convex Hulls. *IEEE Trans. on Image Processing.* 8(7): 934-946.

[24] Yoon, Y. H. and K. H. Jo. 2003. Hands Shape Recognition Using Moment Invariant for The Korean Sign Language Recognition. *Proc. Of Korea-Russia Int. Symp. on Science & Technology.* 2: 308-313.

[25] Zhu, P. and P. M. Chirlian. 1995. On Critical Point Detection of Digital Shapes. *IEEE Trans. on Pattern Analysis and Machine Intelligence.* 17(8): 737-748.